IET Microwaves, Antennas & Propagation

Research Article

IET Journals
The Institution of Engineering and Technology

Application of multi-objective fractional factorial design for ultra-wideband antennas with uniform gain and high fidelity

ISSN 1751-8725
Received on 2nd March 2015
Revised on 12th May 2015
Accepted on 15th June 2015
doi: 10.1049/iet-map.2015.0150
www.ietdl.org

Yen-Sheng Chen ✉

Department of Electronic Engineering, National Taipei University of Technology, Taipei 10608, Taiwan
✉ *E-mail: yschen@ntut.edu.tw*

Abstract: An efficient design methodology is presented for developing ultra-wideband (UWB) antennas with uniform gain and high fidelity. The major challenge for designing UWB antennas is to simultaneously meet all the frequency-domain and time-domain performance criteria including good impedance matching throughout the operational frequencies, relatively uniform gain over the UWB, and high waveform fidelity on pulse-preserving capabilities. If the framework of Pareto-based evolutionary algorithms is adopted, it may require thousands of tests to find an optimum structure due to the blind-search feature. In this study, all the requirements of UWB antenna design can now be efficiently achieved by the proposed methodology, which integrates the processes of fractional factorial design of experiments and Derringer's desirability functions into a multi-objective optimisation technique. The detailed procedure and its capability are demonstrated by an UWB planar monopole antenna design which comprises nine design parameters. By performing merely 64 predefined simulations, the optimum antenna structure is determined with an excellent impedance matching by 2:1 voltage standing wave ratio and a relatively constant gain (2.48–5.04 dBi) over the frequency band of 3.1–10.6 GHz. Meanwhile, the time-domain distortion is greatly reduced in comparison with the reference design which simply optimises the characteristic of impedance matching.

1 Introduction

Recently, there have been increasing research interests in ultra-wideband (UWB) communication systems, and this technology has been deployed in various applications which require short-range transmission with very high data rates. Among these applications, antenna design still remains the most challenging issue in the research of UWB system performance enhancements. Such difficulty results from the complexity that UWB antenna design is a multi-objective (MO) optimisation problem. Specifically, an UWB antenna requires good impedance matching and relatively uniform gain over the targeted frequency band of 3.1–10.6 GHz. Meanwhile, since ultra-short pulses are adopted as the signal waveform, the pulse distortion between the transmitting and receiving signals must be as low as possible. If conventional design methods such as trial-and-error approaches or one-at-a-time parametric studies are applied, they usually have very poor results to simultaneously meet all the performance criteria in a short design cycle. Therefore, it is crucial to develop an efficient and systematic technique for UWB antenna design.

Many optimisation techniques have been applied to the design problem of UWB antennas [1–14]; however, the efficacy and efficiency of these techniques are still insufficient. With regard for efficacy, a number of literatures merely focused on the single-objective optimisation for UWB impedance matching [1–5]. Only some literatures targeted at the MO optimisation for both the wide impedance bandwidth and uniform gain [6–10]; moreover, fewer literatures dealt with impedance matching and signal distortion concurrently [11–14]. To the author's best knowledge, a study that copes with all the requirements – impedance matching, uniformity of gain, and fidelity of time-domain signals – has not yet been much investigated. As for the efficiency, either genetic algorithms [1–4, 7–14] or particle swarm optimisation [5, 6] was applied to the antenna design problem; nevertheless, these Pareto-based evolutionary algorithms usually require hundreds or even thousands of tests due to their blind-search characteristic. No matter what the problem nature is, they just launch a population of candidate solutions, searching the solution domain by executing specific operators until a termination criterion is met. Such a laborious process is so time-consuming that the design cycle is inevitably expanded.

In this paper, MO fractional factorial design (MO-FFD) is applied to the development of UWB antennas. FFD belongs to the class of design of experiments (DOEs), which has been applied to several electromagnetic (EM) problems to study how design parameters influence response variables. These applications include the design of radio-frequency identification tag antennas [15], Baluns [16], flip-chip applications [17], annular ring antennas [18], and patch antennas [19]. Among these applications, DOE is capable of building the response surface model of a design goal, which is the function of design parameters. It is observed that by making use of these response surface models the optimisation procedure can be performed in a simple and inexpensive way; therefore, FFD is integrated with Derringer's desirability functions [20] into a systematic process, and this technique is utilised to cope with all the frequency-domain and time-domain design goals of UWB antennas. The procedure, efficacy, and efficiency will be thoroughly demonstrated. Moreover, the optimised performances supplemented with simulated and measured results will be exhibited.

2 MO-FFD procedure

Unlike the framework of evolutionary algorithms, which regards the design problem as a black box, MO-FFD aims to uncover the black box by approximating the problem with mathematical models. The proposed procedure is arranged by two phases: response surface modelling and MO problem solving. To demonstrate its detailed procedure, let us consider the design problem of an UWB antenna as depicted in Fig. 1. This benchmarking topology consists of a planar monopole antenna and multisection notches at the lower corners fed by a 50 Ω microstrip line. The antenna is developed on a 1.6 mm thick flame retardant 4 (FR4) substrate (dielectric constant $\varepsilon_r = 4.4$ and loss tangent $\tan\delta = 0.02$) with an area of

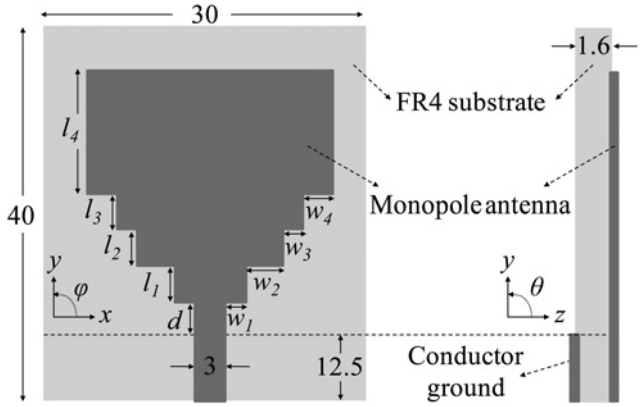

Fig. 1 *Geometry of the benchmarking planar monopole antenna*

$30 \times 40\ \text{mm}^2$. The planar monopole configuration has several advantages such as easy fabrication and azimuthally omni-directional patterns, so the antenna is highly suitable for UWB communication systems [21–24]. However, the gain uniformity and minimised pulse distortion have not yet been systematically met by those earlier attempts; furthermore, the number of design parameters is so large that the design complexity arises if trial-and-error approaches or Pareto-based MO optimisers are used.

2.1 Phase one: response surface modelling

Similar to most of the optimisation methods, MO-FFD begins by identifying the design parameters and the design goals. The design parameters of this topology include the longitudinal lengths of the monopoles l_1, l_2, l_3, and l_4, the transverse widths of the monopoles w_1, w_2, w_3, and w_4, and the distance between the lower edge of the monopole and the upper edge of the truncated ground plane d. The three design goals – minimised reflection coefficients between 3.1 and 10.6 GHz (F_1), uniform peak gains over the targeted frequency band (F_2), and maximised fidelity factors [25] in the E-plane and H-plane (F_3) – are given by

$$\text{minimise } F_1 = \sum_{f \in F_\text{m}} |\Gamma(f)|^3 \tag{1}$$

$$\text{minimise } F_2 = \underset{f \in F_\text{m}}{s.d.}\{G(f)\} \tag{2}$$

$$\text{maximise } F_3 = \sum_{\theta \in \theta_\text{m}} \left[FF(\theta,\ \phi = 0^\circ) + FF(\theta,\ \phi = 90^\circ)\right] \tag{3}$$

where $\Gamma(f)$ and $G(f)$ are the magnitude of reflection coefficient and peak gain at frequency f, respectively; $F_\text{m} = \{3, 4, 5, 6, 7, 8, 9, 10, 10.6\ \text{GHz}\}$ is the set of sampled frequencies. $s.d.\{G(f)\}$ is the sample standard deviation of $G(f)$. $FF(\theta, \varphi)$ is the fidelity factor between the time-domain input signal and the electric field intensity signal measured by a virtual probe situated at the far field along a specified direction (θ, φ); $\theta_\text{m} = \{0^\circ, 30^\circ, 60^\circ, 90^\circ, 120^\circ, 150^\circ, 180^\circ\}$ is the set of sampled directions. It is noted that the power of '3' at (1) is determined by seeking the balance between the degree of wide impedance bandwidth and the degree of good impedance matching. Additional studies on other exponents have been conducted, and the results show that it is difficult to meet the bandwidth requirement by using $\Sigma|\Gamma(f)|^2$.

Table 1 Ranges for the design parameters (millimetres)

Design parameter	Low level (–)	High level (+)
l_1	1.0	4.0
l_2	1.0	4.0
l_3	1.0	4.0
l_4	8.0	12.0
w_1	0.5	3.0
w_2	0.5	3.0
w_3	0.5	3.0
w_4	1.5	4.0
d	0.2	1.2

Once the pre-optimisation process has been performed, MO-FFD purposely varies the design parameters at low level (−) and high level (+) so that their influences can be statistically estimated. Table 1 shows the chosen range of the nine design parameters. Next, a 2^{9-3} FFD of experiment is applied to this design problem. Specifically, d, w_1, l_1, w_2, l_2, and w_3 are chosen as the basic variables, and the associated 2^6 full factorial experiment is constructed. The state of the other three parameters, namely, l_3, w_4, and l_4, are assigned as $l_3 = d \times w_1 \times l_1 \times w_2$, $w_4 = d \times l_1 \times w_2 \times l_2$, and $l_4 = l_1 \times w_2 \times l_2 \times w_3$. As a result, the important main effects of all the design parameters are estimated without confounding with each other, and the precedence of important two-factor interactions can be clarified by the hierarchy principle.

Subsequently, the responses of the resultant 64 antenna structures are tested by computer simulation technology (CST) Microwave Studio full wave analyser. The simulated results are readily transformed to the parameters' effects to see whether the design parameters influence the design goals. More explicitly, the main effect E_i of the design parameter x_i is calculated by subtracting the average response for x_i being low level from the average response for x_i being high level. The two-factor interactions E_{ij} is calculated by subtracting the average main effect E_i for the parameter x_j being low level from the average E_i when x_j being high level. On the basis of such effect computations, 64 estimated effects from the 64 simulations for each design goal are thus obtained. According to the sparsity-of-effects principle, only the significant main effects and two-factor interactions are cast into the response surface models. The inference of significance is drawn by repeated analysis of variance. Afterwards, these significant effects are transformed into the coefficients of the response surface model expressed as (see (4))
(see (5 and 6) at the bottom of the next page)

These response surface models explain the relationship between the design parameters and the design goals. The efficacy of these expressions can be examined by their R^2 value, which represents the percentage of the response variable variation explained by a regression model. The resultant R^2 for F_1, F_2, and F_3 are 0.90, 0.76, and 0.82, respectively, which means that all the models account for over 76% variability in this design problem. Therefore, these models provide good prediction on the antenna performances by substituting a specific combination of design parameters. Moreover, they can be used to synthesise the desired antenna performances.

$$\begin{aligned} F_1 = {} & 0.55 + 0.07\left(\frac{w_4 - 2.75}{1.25}\right) - 0.16\left(\frac{w_1 - 1.75}{1.25}\right) - 0.04\left(\frac{d - 0.7}{0.5}\right) - 0.06\left(\frac{l_3 - 2.5}{1.5}\right) + 0.04\left(\frac{l_2 - 2.5}{1.5}\right) - 0.14\left(\frac{w_2 - 1.75}{1.25}\right) \\ & + 0.17\left(\frac{l_1 - 2.5}{1.5}\right) - 0.09\left(\frac{w_1 - 1.75}{1.25}\right)\left(\frac{d - 0.7}{0.5}\right) - 0.05\left(\frac{w_1 - 1.75}{1.25}\right)\left(\frac{l_2 - 2.5}{1.5}\right) + 0.06\left(\frac{w_1 - 1.75}{1.25}\right)\left(\frac{w_2 - 1.75}{1.25}\right) \\ & - 0.07\left(\frac{w_1 - 1.75}{1.25}\right)\left(\frac{l_1 - 2.5}{1.5}\right) - 0.09\left(\frac{l_2 - 2.5}{1.5}\right)\left(\frac{w_2 - 1.75}{1.25}\right) \end{aligned} \tag{4}$$

IET Microw. Antennas Propag., 2015, Vol. 9, Iss. 15, pp. 1667–1672

2.2 Phase two: MO problem solving

To simultaneously optimise the three design goals, the design problem is formulated into a constrained programming problem

$$\text{find: } \boldsymbol{x}^* = \arg\min_{\boldsymbol{x}} F_2(\boldsymbol{x})$$
$$\text{subject to: } \begin{cases} F_1(\boldsymbol{x}) \le 0.24 \\ F_3(\boldsymbol{x}) \ge 0.8 \\ \boldsymbol{x} \in \{-1 \le x_i \le 1\} \end{cases} \tag{7}$$

where $\boldsymbol{x}$ is the combination of all the design parameter x_i which has been normalised from the range in Table 1 to [–1, 1]. To cope with such a non-linear and non-convex constrained problem, a series of feasible solutions satisfying the constraints are first obtained by a direct-search manner, and these feasible solutions are further ranked by Derringer's desirability functions. More explicitly, for the minimisation-oriented objective F_1, its value is transformed into a dimensionless desirability d_1 by

$$d_1 = \begin{cases} 1, & F_1 < 0.05 \\ \dfrac{0.24 - F_1}{0.24 - 0.05}, & 0.05 \le F_1 \le 0.24 \\ 0, & F_1 > 0.24 \end{cases} \tag{8}$$

The functional graph of (8) is shown in Fig. 2*a*. It indicates that $d_1 = 0$ if F_1 is worst than 0.24; on the other hand, if F_1 is better than 0.05, then $d_1 = 1$. Similarly, for the other minimisation-oriented objective F_2, its value is transformed into d_2 by

$$d_2 = \begin{cases} 1, & F_2 < 0.5 \\ \dfrac{0.8 - F_2}{0.8 - 0.5}, & 0.5 \le F_2 \le 0.8 \\ 0, & F_2 > 0.8 \end{cases} \tag{9}$$

As can be observed in Fig. 2*b* the value of F_2 is converted into a dimensionless d_2 that varies between 0 and 1. On the other hand, for the maximisation-oriented objective F_3, the response is transformed by

$$d_3 = \begin{cases} 0, & F_3 < 0.8 \\ \dfrac{F_3 - 0.8}{0.85 - 0.8}, & 0.8 \le F_3 \le 0.85 \\ 1, & F_3 > 0.85 \end{cases} \tag{10}$$

The functional graph of (10) is shown in Fig. 2*c*, which indicates that if F_3 is smaller than the acceptable lower bound 0.8, then $d_3 = 0$; in contrast, if F_3 is larger than a satisfactory threshold 0.85, then $d_3 = 1$.

After transforming the response of each design goal into the individual desirability, the overall desirability D for a design is defined as the geometric means of d_1, d_2, and d_3; the design having the largest D is thus the optimal. The associated parameters

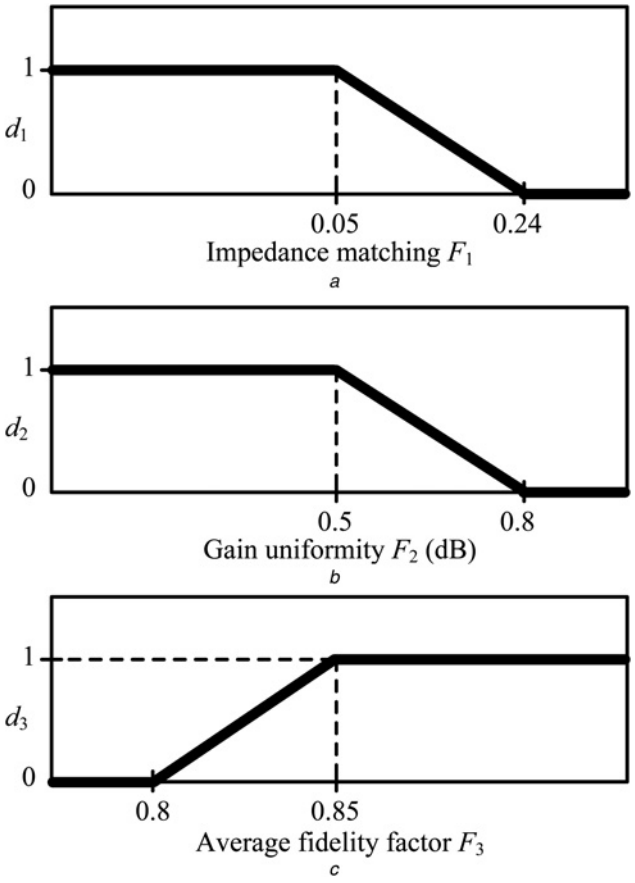

Fig. 2 *Individual desirability function for the objective is*
a Minimisation of F_1
b Minimisation of F_2
c Maximisation of F_3

for this optimised UWB antenna design are $l_1 = 2.38$ mm, $l_2 = 4$ mm, $l_3 = 4$ mm, $l_4 = 11.3$ mm, $w_1 = 2.98$ mm, $w_2 = 2.94$ mm, $w_3 = 3$ mm, $w_4 = 4$ mm, and $d = 0.52$ mm. The design is then verified by the CST, and the simulated responses are $F_1 = 0.02$, $F_2 = 0.72$ dB, and $F_3 = 0.84$. Clearly, with the design methodology presented above, an optimised impedance bandwidth along with a relatively uniform gain and high fidelity is obtained in a very systematic and efficient manner.

3 Numerical results

To facilitate assessing the MO optimisation capability of MO-FFD, two reference antennas were developed for comparison purpose. The first reference antenna is a single-objective UWB antenna designed by optimising the impedance-matching criterion (1) only; neither

$$F_2(\text{dB}) = 0.97 - 0.05\left(\frac{w_4 - 2.75}{1.25}\right) - 0.04\left(\frac{w_1 - 1.75}{1.25}\right) + 0.02\left(\frac{d - 0.7}{0.5}\right) - 0.05\left(\frac{w_3 - 1.75}{1.25}\right) - 0.04\left(\frac{w_2 - 1.75}{1.25}\right) - 0.03\left(\frac{w_4 - 2.75}{1.25}\right) \times \left(\frac{w_1 - 1.75}{1.25}\right) - 0.02\left(\frac{w_4 - 2.75}{1.25}\right)\left(\frac{l_2 - 2.5}{1.5}\right) - 0.03\left(\frac{w_1 - 1.75}{1.25}\right)\left(\frac{l_2 - 2.5}{1.5}\right) - 0.02\left(\frac{w_1 - 1.75}{1.25}\right)\left(\frac{w_2 - 1.75}{1.25}\right) \tag{5}$$

$$F_3 = 0.74 - 0.06\left(\frac{l_4 - 10}{2}\right) - 0.02\left(\frac{w_1 - 1.75}{1.25}\right) - 0.01\left(\frac{l_3 - 2.5}{1.5}\right) - 0.02\left(\frac{w_3 - 1.75}{1.25}\right) - 0.02\left(\frac{w_2 - 1.75}{1.25}\right) + 0.02\left(\frac{w_4 - 2.75}{1.25}\right)\left(\frac{l_4 - 10}{2}\right) + 0.03\left(\frac{w_4 - 2.75}{1.25}\right)\left(\frac{l_3 - 2.5}{1.5}\right) + 0.01\left(\frac{l_4 - 10}{2}\right)\left(\frac{w_1 - 1.75}{1.25}\right) \tag{6}$$

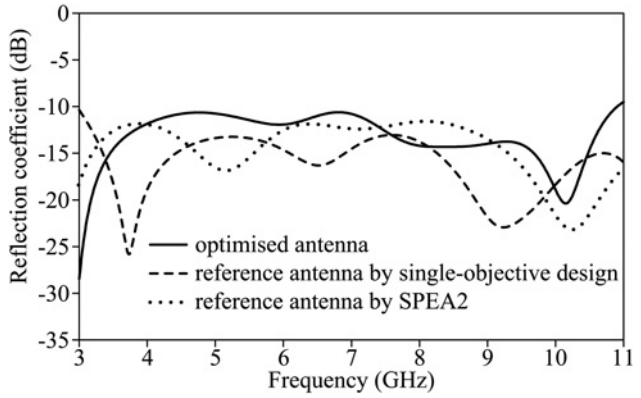

Fig. 3 *Simulated reflection coefficients of the optimised antenna and those of the reference antennas*

uniform gain (2) nor high fidelity (3) was included in the design goals. The other reference antenna was constructed by strength Pareto evolutionary algorithm 2 (SPEA2) [26]. The design parameters were also $\{d, w_1, l_1, w_2, l_2, w_3, l_3, w_4, l_4\}$, and the fitness functions were again the expressions (1)–(3). More explicitly, SPEA2 used a real-number coding, performing 60 iterations with a population size of 50 chromosomes. The mutation was performed by adding noises to chromosomes with a probability of 0.02, and the cross-over was done by the blend cross-over (BLX)-α with $\alpha = 0.5$ and a probability of 0.5 [27]. As a result, a series of satisfactory designs on the non-dominated solution set were obtained, and the optimum design can be selected out of the Pareto front.

First of all, the simulated reflection coefficients of the optimised antenna and the two reference antennas are shown in Fig. 3. The performances between the three antennas are comparable; all the antennas meet the 2 : 1 VSWR requirement in the frequency band of 3.1–10.6 GHz. Nonetheless, if the second criterion – uniformity of peak gain – is further considered, the peak gains of the optimised antenna are more uniform than those of the two reference antennas over the targeted frequency band. The simulated peak gains are shown and compared in Fig. 4. The peak gains of the optimised antenna are between 2.48 and 5.04 dBi; in contrast, without the treatment of gain uniformity by (2), the peak gain of the first reference antenna fluctuates within a much wider range (1.79–6.03 dBi). Besides, the second reference antenna designed by SPEA2 still has a larger range of peak gain variation (2.02–5.61 dBi). Finally, the fidelity factors obtained for the optimised design are shown and compared with those for the two reference designs in Fig. 5. It can be seen that with the treatment of pulse preserving by (3), MO-FFD greatly improves the fidelity factor in most of the directions. More significantly, all the good

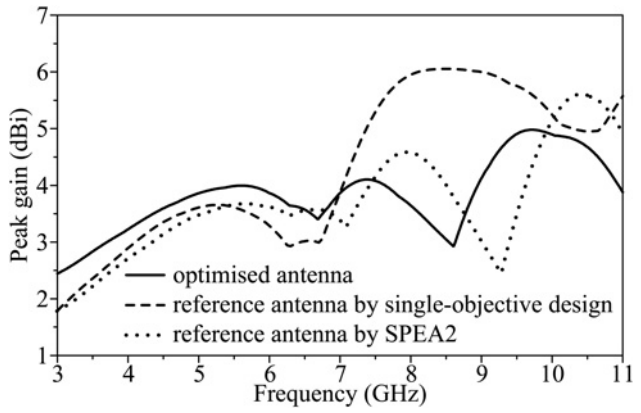

Fig. 4 *Simulated peak gains of the optimised antenna and those of the reference antennas*

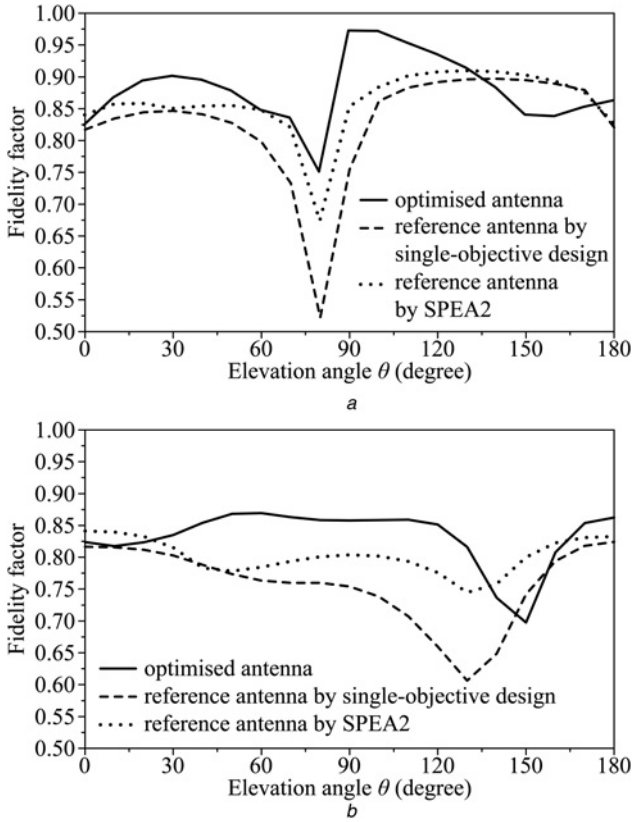

Fig. 5 *Simulated fidelity factors of the optimised antenna and those of the reference antennas in the*

a E-plane
b H-plane

performances including good impedance matching, uniform gains, and high fidelity factors are simultaneously obtained with merely 64 tests. In contrast, MO evolutionary algorithms such as SPEA2 are very time-consuming due to the necessity of numerous iterations with a large population size. In sum, MO-FFD reduces the design cycle by 97%.

4 Experimental verification

For verification purpose, the optimised UWB antenna structure was fabricated and tested. A 50 Ω SubMiniature version A connector was mounted to the test piece to measure the antenna performances; moreover, the mismatch effect between the SMA connector and the antenna structure was modelled in the following high-frequency structure simulator simulations. The simulated and measured reflection coefficients of the optimised antenna are shown in Fig. 6. They exhibit good agreement in general. The measured results confirm that the required impedance matching is achieved over the interested frequency band.

The simulated and measured peak antenna gains including mismatching loss are provided in Fig. 7. The measured gain variation is <2.69 dB (2.51–5.21 dBi), which further verifies that the EM radiation is quite stable throughout the operational frequencies. In addition, the simulated and measured gain patterns in the *E* and *H* planes at 3.5, 6.5, and 10.5 GHz are also exhibited in Fig. 8. Good agreement between the simulated and measured results can be observed, with the exception of slight deviation at nearby $\theta = 180°$ due to the environmental constraint of the anechoic chamber. Clearly, the EM radiation demonstrates dipole-wise patterns. Nearly, omni-directional radiation characteristics are observed; therefore, the optimised antenna is highly suitable for UWB communication systems.

IET Microw. Antennas Propag., 2015, Vol. 9, Iss. 15, pp. 1667–1672

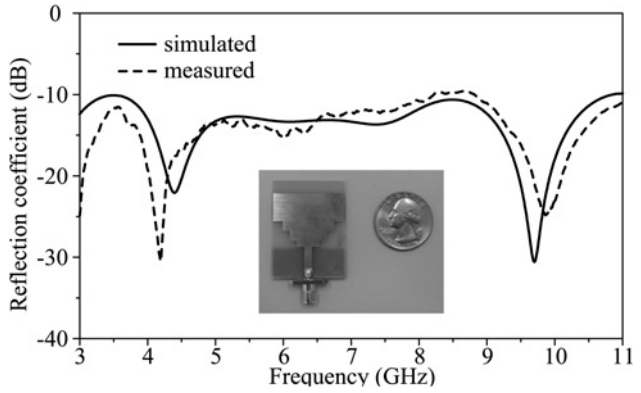

Fig. 6 *Measured and simulated reflection coefficients of the optimised antenna. Shown in the inset is the photograph of the fabricated prototype*

Finally, time-domain characteristics were also measured and tested. A post-processed measurement was adopted to evaluate the system fidelity factor [28, 29]. Two identical optimised UWB antennas were separated by 400 mm inside an anechoic chamber and assigned as the transmitting and receiving antennas, respectively. The transmitting signal was selected as the fourth-derivative of a Gaussian function

$$s_i(t) = A\left(3 - 6\left(\frac{4\pi}{T_{au}^2}\right)t^2 + \left(\frac{4\pi}{T_{au}^2}\right)^2 t^4\right) \times e^{-2\pi\left(\frac{t}{T_{au}}\right)^2} \text{ (V/m)} \quad (11)$$

where $A = 0.1$ and $T_{au} = 0.175$ ns. After measuring the normalised transfer function between the two antennas by a vector network analyser, the output spectrum was computed by the multiplication of the normalised transfer function and the Fourier transform of the input signal. This output spectrum was readily converted into a time-domain receiving signal by taking the inverse Fourier transform. Finally, the system fidelity factor was evaluated by the correlation coefficient between the transmitting and receiving signals

$$F(\theta,\ \phi) = \max_{\tau}\left(\frac{\left|\int_{-\infty}^{\infty} s_i(t)s_o(t+\tau,\ \theta,\ \phi)\,dt\right|}{\sqrt{\int_{-\infty}^{\infty} s_i(t)^2\,dt \int_{-\infty}^{\infty} s_o(t+\tau,\ \theta,\ \phi)^2\,dt}}\right) \quad (12)$$

where $s_i(t)$ and $s_o(t)$ are the input and output signals, respectively. The measured fidelity factors for the optimised antenna system in the face-to-face orientation are shown in Fig. 9. The average fidelity factors for the E and H planes are 0.86 and 0.81, respectively. Both planes show a good fidelity patterns. This further validates that the optimised antenna does not distort the transmitted signal significantly.

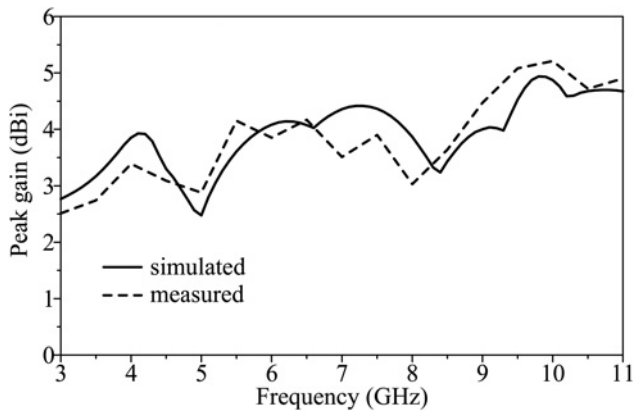

Fig. 7 *Measured and simulated peak antenna gains of the optimised antenna (with mismatching loss included)*

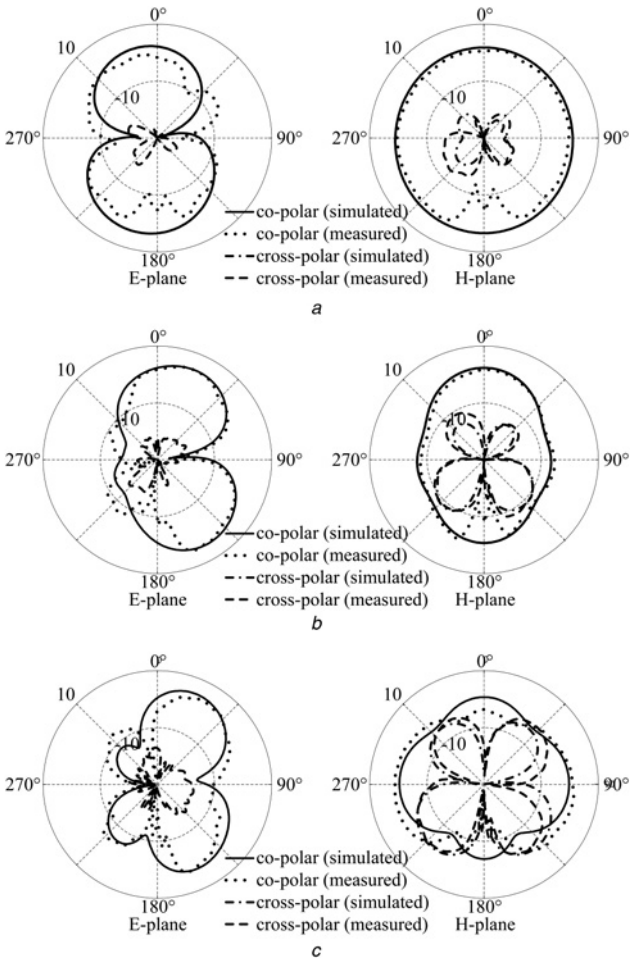

Fig. 8 *Measured and simulated radiation patterns of the optimised antenna at*

a 3.5 GHz
b 6.5 GHz
c 10.5 GHz

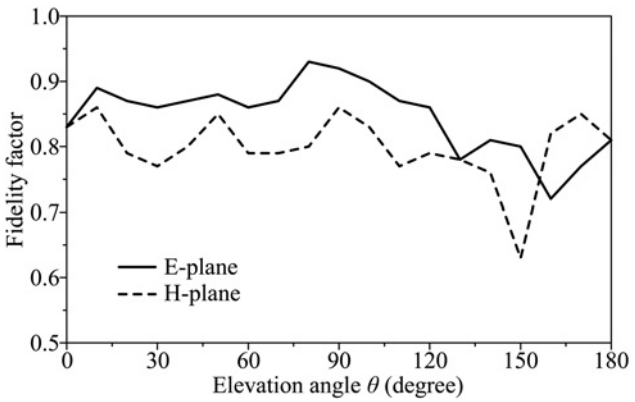

Fig. 9 *Measured system fidelity factors for two optimised antennas in the face-to-face orientation*

5 Conclusion

This paper presents an efficient methodology aimed for optimising all the design requirements of UWB antennas. The significance of

MO-FFD is two-fold. First, this technique greatly reduces the design cycle; by applying MO-FFD to the design problem of a planar monopole antenna, the optimised antenna structure is determined with merely 64 tests even though the structure has nine design parameters. Second, this technique is capable of overcoming all the performance criteria of UWB antennas. Although the requirements of impedance matching, uniformity of peak gain, and the fidelity of time-domain signals are imposed into the design process, MO-FFD obtains an optimum design with a VSWR < 2 bandwidth from 3.1 to 10.6 GHz, while maintaining a relatively constant peak gain with slight variations (2.48–5.04 dBi) over the targeted frequency band; meanwhile, the time-domain fidelity factors are greatly enhanced. As the optimised antenna is operated in transmitting mode, using an ideal probe having an isotropic pattern as the receiving antenna shows enhanced fidelity factors in most of the directions; the average fidelity factors in the *E* and *H* planes are 0.88 and 0.84, respectively, indicating that the correlation between the transmitting and receiving signals is very high. On the other hand, if the receiving antenna is replaced by the optimised antenna having dipole-wise patterns, the average fidelity factors slightly decrease (average *E*-plane and *H*-plane fidelity factors are 0.86 and 0.81, respectively), but the signal correlation between the transmitting and receiving pulses is still high enough for UWB applications. These results confirm that the MO-FFD is particularly suitable for UWB antenna design.

6 References

1 Kerkhoff, A.J., Rogers, R.L., Ling, H.: 'Design and analysis of planar monopole antennas using a genetic algorithm approach', *IEEE Trans. Antennas Propag.*, 2004, **52**, (6), pp. 1768–1771

2 Kim, J., Yoon, T., Kim, J., *et al.*: 'Design of an ultra wide-band printed monopole antenna using FDTD and genetic algorithm', *IEEE Microw. Wirel. Compon. Lett.*, 2005, **15**, (6), pp. 395–397

3 John, M., Ammann, M.J.: 'Wideband printed monopole design using a genetic algorithm', *IEEE Antennas Wirel. Propag. Lett.*, 2007, **6**, pp. 447–449

4 John, M., Ammann, M.J.: 'Antenna optimisation with a computationally efficient multiobjective evolutionary algorithm', *IEEE Trans. Antennas Propag.*, 2009, **57**, (1), pp. 260–263

5 Li, Y.-L., Shao, W., You, L., *et al.*: 'An improved PSO algorithm and its application to UWB antenna design', *IEEE Antennas Wirel. Propag. Lett.*, 2013, **12**, pp. 1236–1239

6 Martín, J.E., Pantoja, M.F., Bretones, A.R.: 'Exploration of multi-objective particle swarm optimisation on the design of UWB antennas'. Proc. Third European Conf. on Antennas and Propagation, Berlin, Germany, March 2009, pp. 561–565

7 Yang, X.-S., Ng, K.T., Yeung, S.H., *et al.*: 'Jumping genes multiobjective optimisation scheme for planar monopole ultrawideband antenna', *IEEE Trans. Antennas Propag.*, 2008, **56**, (12), pp. 3659–3666

8 Tian, B., Li, Z., Wang, C.: 'Boresight gain optimisation of an UWB monopole antenna using FDTD and genetic algorithm'. Proc. Int. Conf. Ultra-Wideband (ICUWB), Nanjing, China, September 2010, pp. 1–4

9 Liu, C.-W., Chen, C.-C.: 'A UWB three-layer dielectric rod antenna with constant gain, pattern, and phase center', *IEEE Trans. Antennas Propag.*, 2012, **60**, (10), pp. 4500–4508

10 Zhao, J., Psychoudakis, D., Chen, C.-C., *et al.*: 'Design optimisation of a low-profile UWB body-of-revolution monopole antenna', *IEEE Trans. Antennas Propag.*, 2012, **60**, (12), pp. 5578–5586

11 Telzhensky, N., Leviatan, Y.: 'Novel method of UWB antenna optimisation for specific input signal forms by means of genetic algorithm', *IEEE Trans. Antennas Propag.*, 2006, **54**, (8), pp. 2216–2225

12 Chamaani, S., Mirtaheri, S.A., Paran, K., *et al.*: 'Coplanar waveguide-fed ultra wideband planar monopole antenna optimisation', *IET Microw. Antennas Propag.*, 2010, **4**, (9), pp. 1264–1274

13 Dumoulin, A., John, M., Ammann, M.J., *et al.*: 'Optimised monopole and dipole antennas for UWB asset tag location systems', *IEEE Trans. Antennas Propag.*, 2012, **60**, (6), pp. 2896–2904

14 Toccafondi, A., Garufo, A., Giovampaola, C.D.: 'Coplanar waveguide-fed compact antenna for UWB RFID applications'. Proc. Seventh European Conf. on Antennas and Propagation, Gothenburg, Sweden, April 2013, pp. 3048–3049

15 Yang, L., Martin, L.J., Staiculescu, D., *et al.*: 'Conformal magnetic composite RFID for wearable RF and bio-monitoring applications', *IEEE Trans. Microw. Theory Tech.*, 2008, **56**, (12), pp. 3223–3230

16 Staiculescu, D., Bushyager, N., Obatoyinbo, A., *et al.*: 'Design and optimization of 3-D compact stripline and microstrip Bluetooth/WLAN Balun architectures using the design of experiments technique', *IEEE Trans. Antennas Propag.*, 2005, **53**, (5), pp. 1805–1812

17 Staiculescu, D., Laskar, J., Tentzers, M.M.: 'Design rule development for microwave flip-chip applications', *IEEE Trans. Microw. Theory Tech.*, 2000, **48**, (9), pp. 1476–1481

18 Maldonado-Vargas, J., Rodríguez-Solís, R.A.: 'Analysis of a cavity backed annular slot ring antenna using design of experiment techniques'. IEEE AP-S Int. Symp. and URSI Radio Science Meeting, Memphis, TN, July 2014, pp. 1501–1502

19 Roy, A., Paul, S., Shamsuzzaman, A.S.M., *et al.*: 'Design of optimum antenna system for maximum power transfer using statistical design of experiment approach'. PIERS Proc., Beijing, China, March 2009, pp. 1624–1628

20 Derringer, G., Suich, R.: 'Simultaneous optimisation of several response variables', *J. Qual. Technol.*, 1980, **12**, (4), pp. 214–219

21 Abbosh, A.M., Bialkowski, M.E.: 'Design of ultrawideband planar monopole antennas of circular and elliptical shape', *IEEE Trans. Antennas Propag.*, 2008, **56**, (1), pp. 17–23

22 Behdad, N., Sarbandi, K.: 'A compact antenna for ultrawide-band applications', *IEEE Trans. Antennas Propag.*, 2005, **53**, (7), pp. 2185–2192

23 Liang, J., Guo, L., Chiau, C.C., *et al.*: 'Study of CPW-fed circular monopole antenna for ultra wideband applications', *IEE Proc. Microw. Antenna Propag.*, 2005, **152**, (6), pp. 520–526

24 Lizzi, L., Viani, F., Azaro, R., *et al.*: 'Optimisation of a spline-shaped UWB antenna by PSO', *IEEE Antennas Wirel. Propag. Lett.*, 2007, **6**, pp. 182–185

25 Lamensdorf, D., Susman, L.: 'Baseband-pulse-antenna techniques', *IEEE Antennas Propag. Mag.*, 1994, **36**, (1), pp. 20–30

26 Zitzler, E., Laumanns, M., Thiele, L.: 'SPEA2: improving the strength Pareto evolutionary algorithm'. Technical Report, 103, Computer Engineering and Networks Laboratory (TIK), Swiss Federal Institute of Technology (ETH), Zurich, Switzerland, May 2001

27 Eshelman, L.J., Schaffer, J.D.: 'Real-coded genetic algorithms and interval-schemata'. Foundations of Genetic Algorithms 2, San Mateo, CA: Morgan Kaufmann, 1993, pp. 187–202

28 Quintero, G., Zürcher, J.-F., Skrivervik, A.K.: 'System fidelity factor: a new method for comparing UWB antennas', *IEEE Trans. Antennas Propag.*, 2011, **59**, (7), pp. 2502–2512

29 Ma, T.-G., Jeng, S.-K.: 'Planar miniature tapered-slot-fed annular slot antennas for ultrawide-band radios', *IEEE Trans. Antennas Propag.*, 2005, **53**, (3), pp. 1194–1202